An allosteric model of circadian KaiC phosphorylation

Supporting Information

Jeroen S. van Zon, David K. Lubensky, Pim R. H. Altena,
and Pieter Rein ten Wolde

Contents

In this *Supporting Information*, we provide background information on our model of the *in vitro* Kai system and the calculations that we have performed. We will closely follow the outline of the main text.

1 Allosteric Model

In this section, we discuss in more detail the allosteric model of section I of the main text. We first present a statistical-mechanical description of the allosteric model. This allows us to describe the thermodynamics of the phosphorylation cycle. We then present a model based on concepts of transition state theory that allows us to describe the *dynamics* of the phosphorylation cycle, in particular the dynamics of the conformational transtions. Lastly, we briefly discuss how we have performed the simulations on the model in Fig.1B of the main text, the results of which are shown in Fig.1C of the main text.

1.1 Thermodynamics: A statistical-mechanical model

The allosteric model relies on the following key assumptions:

1. Each of the $N = 6$ monomers of a hexamer is either in an active or in an inactive conformational state.
2. The conformations of the monomers are strongly coupled, such that all monomers of a hexamer are in the same conformational state at all times.
3. Both in the active and inactive state, monomers can be (de)phosphorylated and (un)bind nucleotides. We assume that nucleotides have a higher affinity for monomers in the active state than for those in the inactive state. Consequently, nucleotide binding enhances the stability of the active state with respect to the inactive one. In contrast, we assume that phosphorylation favors the inactive state.
4. Nucleotide exchange is faster than phosphorylation and therefore in thermodynamic equilibrium on the time scale of phosphorylation.

The model makes the following further assumptions that are of secondary importance:

1. Each monomer has two phosphorylation states, phosphorylated and unphosphorylated. Each hexamer thus has $N = 6$ phosphorylation sites.
2. Phosphorylation of the different monomers of a hexamer occurs sequentially around the hexamer.
3. The unphosphorylated monomers can bind ATP, while the phosphorylated monomers can bind ADP.

This leads to the following partition function for a hexamer that it is in a conformational state α, at phosphorylation level p, with q ATP and r ADP molecules bound:

$$\begin{aligned} Z^{\alpha}(p,q,r) &= e^{-\beta N E_{\mathrm{m}}^{\alpha}} \binom{N-p}{q} \left([\mathrm{ATP}]/K_{\mathrm{D}}^{\alpha,\mathrm{T}}\right)^{q} \times \\ &\quad \left([\mathrm{Pi}]/K_{\mathrm{D}}^{\alpha,\mathrm{P}}\right)^{p} \binom{p}{r} \left([\mathrm{ADP}]/K_{\mathrm{D}}^{\alpha,\mathrm{D}}\right)^{r}. \end{aligned} \tag{1}$$

Here, β is the inverse temperature, E_{m}^{α} is the energy of an unphosphorylated monomer in state α (with no nucleotide bound), and $K_{\mathrm{D}}^{\alpha,\mathrm{s}}$ is the dissociation constant for the binding of species s to the hexamer in state α; T denotes ATP, D ADP, and P a phosphate group Pi. Since nucleotide exchange is assumed to be fast, it is meaningful to integrate over the number of nucleotides. This yields the following partition function for a hexamer in state α with phosphorylation level p:

$$\begin{aligned} Z^{\alpha}(p) &= e^{-\beta N E_{\mathrm{m}}^{\alpha}} \left(1 + [\mathrm{ATP}]/K_{\mathrm{D}}^{\alpha,\mathrm{T}}\right)^{N-p} \times \\ &\quad \left[[\mathrm{Pi}]/K_{\mathrm{D}}^{\alpha,\mathrm{P}} \left(1 + [\mathrm{ADP}]/K_{\mathrm{D}}^{\alpha,\mathrm{D}}\right)\right]^{p}. \end{aligned} \tag{2}$$

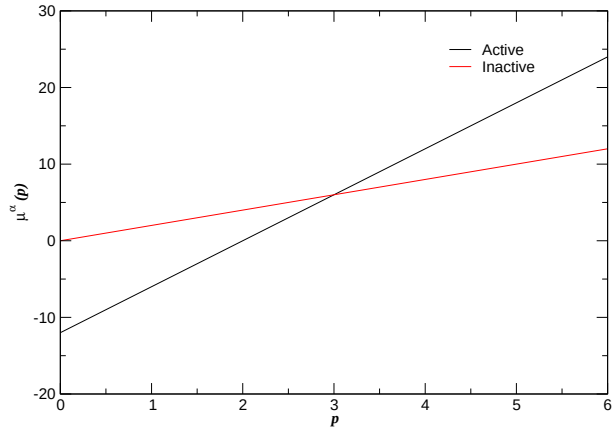

Figure 1: The chemical potential of a KaiC hexamer as a function of the phosphorylation level p, for both the active and inactive conformational state, and for the symmetric model of Fig.1A in the main text. The chemical potential $\mu^\alpha(p)$ is given by Eq. 3.

The (excess) chemical potential of a hexamer in conformational state α at phosphorylation level p is given by

$$\mu^\alpha(p) = -k_{\rm B}T \ln[Z^\alpha(p)]. \tag{3}$$

We stress that the chemical potential of a KaiC hexamer depends upon the chemical potentials (the concentrations) of the nucleotides: $\mu^\alpha(p) = \mu^\alpha(p; \mu^{\rm T}, \mu^{\rm D}, \mu^{\rm P})$.

We will now consider the symmetric model of Fig.1A of the main text. In this model, the energy levels of the active and inactive conformational state are mirror images of each other. This is for reasons of clarity, and not because it is essential. In fact, the full model of section III is asymmetric, with the active state being more stable than the inactive one.

Fig. 1 shows the chemical potentials of a KaiC hexamer in the active and inactive state, respectively, as a function of the phosphorylation level, for the energy diagram shown in Fig.1A of the main text. Here, $\mu^\alpha(p=6) - \mu^\alpha(p=0)$ corresponds to the free-energy change upon fully phosphorylating a KaiC hexamer in conformational state α at constant chemical potentials of the ATP, ADP and Pi molecules, but *without* an ATP hydrolysis reaction (we thus consider the reaction $\mathrm{KaiC} + \mathrm{Pi} \rightarrow \mathrm{KaiCPi}$) . It is seen that the free energy increases markedly for both conformational states, meaning that the probability that a hexamer would fully phosphorylate spontaneously, is essentially zero. Indeed, the essence of our allosteric model is that in the active conformational state, the energy from ATP hydrolysis is used to phosphorylate the KaiC hexamer, while in the inactive state dephosphorylation occurs spontaneously.

When ATP is hydrolyzed to p-fold phosphorylate a single KaiC hexamer in the active state, the total change in free energy of the system is

$$\Delta G^{\mathrm{A}}(p) = \mu^{\mathrm{A}}(p) - \mu^{\mathrm{A}}(0) + p(\mu^{\mathrm{D}} + \mu^{\mathrm{P}} - \mu^{\mathrm{T}}), \tag{4}$$

where $\mu^{\mathrm{A}}(p)$ is given by Eq. 3. If in the active state binding of both ADP and ATP is strong (i.e. $[\mathrm{ADP}]/\mathrm{K}_{\mathrm{D}}^{\mathrm{A,ADP}}, [\mathrm{ATP}]/\mathrm{K}_{\mathrm{D}}^{\mathrm{A,ATP}} \gg 1$), then the above expression reduces to

$$\begin{aligned} \Delta G^{\mathrm{A}}(p) &= p(-\Delta G^{\mathrm{A,T}} + \Delta G^{\mathrm{A,P}} + \Delta G^{\mathrm{A,D}} + \Delta G_{\mathrm{hydro}}) \\ &= p\Delta G^{\mathrm{A}}_{\mathrm{m;AATP}\rightarrow\mathrm{A_pADP}}. \end{aligned} \tag{5}$$

Here, $\Delta G^{\alpha,s} = +k_{\mathrm{B}}T \ln K_{\mathrm{D}}^{\alpha,s}$ is the binding free energy of species s and $\Delta G_{\mathrm{hydro}}$ is the standard reaction free energy of an ATP hydrolysis reaction. The overall free energy change $\Delta G^{\mathrm{A}}(p)$ corresponds to that of p phosphotransfer reactions $\mathrm{AATP} \rightarrow \mathrm{A_pADP}$ on the active KaiC hexamer (A denotes a subunit in the active state). The free-energy change be understood by noting that in the limit of strong nucleotide binding considered here, the unphosphorylated monomers are essentially always occupied by ATP, while the phosphorylated monomers are essentially always occupied by ADP; see also Fig.1A of the main text.

Fig. 2 shows the free energy of the system in the presence of ATP hydrolysis. In the active conformational state, KaiC binds ATP. ATP hydrolysis then drives the phosphorylation of the hexamer, and the reduction in free energy of the whole system is given by Eq. 5. When the hexamer is (nearly) fully phosphorylated, it flips to the inactive conformational state. In the inactive state, nucleotide binding is weak and, as a result, ADP is released. The hexamer now dephosphorylates spontaneously; since nucleotide binding is weak, the free-energy change is given by $6k_{\mathrm{B}}T \ln\left[[\mathrm{Pi}]/K_{\mathrm{D}}^{\mathrm{I,P}}\right]$ (see Eqs. 2 and 3). At low phosphorylation levels, the inactive hexamer flips back towards the active conformational state. KaiC rebinds ATP and the phosphorylation cycle starts over again. After one full phosphorylation cycle, the free energy of the system has been reduced by the free-energy change corresponding to 6 ATP hydrolysis reactions: $\Delta G = 6\left(\Delta G_{\mathrm{hydro}} + k_{\mathrm{B}}T \ln\left([\mathrm{ADP}][\mathrm{Pi}]/[\mathrm{ATP}]\right)\right)$.

1.2 Dynamics: a transition-state theory of the conformational transitions

So far, we have discussed the thermodynamics of the phopshorylation cycle. We will now discuss the *dynamics* of the cycle, in particular the dynamics of the conformational transitions. This is important, because while the large amplitude oscillations as observed experimentally require that the hexamers should not flip at intermediate phopshorylation levels, the stability of one conformational state with respect to that of the other, does change in sign at intermediate phosphorylation levels: in the symmetric model considered here and in Fig.1A of the main text, the active state is more stable for $p < 3$, while the inactive state is more stable for $p > 3$. How can we explain that the conformational transitions

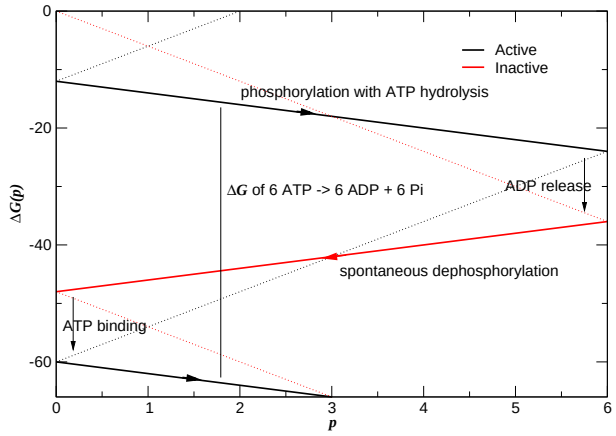

Figure 2: The free energy of the system as a function of the phosphorylation level in the presence of ATP hydrolysis for the symmetric model of Fig.1A in the main text. The solid lines denote the path of the system. Driven by ATP hydrolysis, a KaiC hexamer is phosphorylated in the active state. When the KaiC hexamer is (nearly) fully phosphorylated, it flips from the active to the inactive conformational state. In the inactive state, ADP is released and the hexamer dephosphorylates spontaneously. At low phosphorylation levels, the hexamer flips back to the active state. The active hexamer rebinds ATP and the phosphorylation cycle starts over again. The dotted lines correspond to driven phosphorylation of inactive KaiC and spontaneous dephosphorylation of active KaiC.

predominantly occur when the hexamers are either nearly fully phosphorylated or fully unphosphorylated?

This is a difficult question to answer, because it requires knowledge of the microscopic dynamics of the transition paths between the conformational states. However, if we assume that nucleotide binding is an important component of the reaction coordinate that describes the conformational transitions, then we can make an estimate of the flipping rates using a mesoscopic model based on concepts from transition-state theory [1].

If nucleotide binding contributes to the reaction coordinate of the conformational transitions, then we cannot integrate it out as we have done so far. To derive the flipping rates, we start by considering the free-energy difference between two conformational states with the same number of nucleotides bound:

$$\Delta G(p,q,r) = N\Delta E_{\rm m} + p\Delta E_p + q\Delta E_{\rm T} + r\Delta E_{\rm D}. \qquad (6)$$

Here, $\Delta E_{\rm m} = E_{\rm m}^{\rm A} - E_{\rm m}^{\rm I}$ and $\Delta E_{\rm s} = k_{\rm B}T \ln K_{\rm D}^{\rm A,s}/K_{\rm D}^{\rm I,s}$. If we assume, for simplicity, that the model is symmetric, $\Delta E_{\rm m} = 0$, and that the difference in binding energy between the active and inactive state is the same for ATP and ADP,

$\Delta E_{\rm T} = \Delta E_{\rm D} = \Delta E_{\rm T/D}$, then the above expression reduces to:

$$\Delta G(p,n) = p\Delta E_p + n\Delta E_{\rm T/D}, \tag{7}$$

where n is the number of nucleotides that are bound. We iterate that phosphorylation favors the inactive state, and hence $\Delta E_{\rm p} > 0$, while nucleotide binding favors the active state, $\Delta E_{\rm T/D} < 0$. We can use the above expression to estimate the flipping rate if we assume that nucleotide binding is the dominant reaction coordinate for the flipping process.

This is illustrated in Figs. 3 and 4, for the case $|\Delta E_p| = -|\Delta E_n|$. Fig. 3 shows a sketch of the free-energy surface $\Delta G(p=3,n,c)$ of a three-fold phosphorylated hexamer as a function of the number of bound nucleotides, n, and as a function of an order parameter that describes the conformational state of the hexamer, c; the parameter c is zero if the hexamer is in the inactive state and one if it is in the active state. Clearly, we do not know what would be the best order parameter to describe the conformational transition, let alone what the free energy would be as a function of this order parameter for different values of n. Nevertheless, we do have some knowledge of the free-energy surface: we know how the free energy $\Delta G(p,n,c)$ changes as a function of n for $c = 0$ and for $c = 1$ – this is given by the free energy of nucleotide binding to the inactive and active state, respectively; this free energy is related to the log of the partition function in Eq. 1. We therefore make the minimal assumption that the free-energy surface $\Delta G(p,n,c)$ is given by a linear interpolation between the two functions $\Delta G(p,n,0)$ and $\Delta G(p,n,1)$. This leads to the surface shown in Fig. 3.

In the active state, nucleotides bind the hexamer very strongly and, consequently, $n \approx 6$, while in the inactive state nucleotides bind the hexamer rather weakly and $n \approx 0$. The two (meta)stable states of the hexamer are thus the active state with six nucleotides bound and the inactive state with no nucleotides bound. These two states are separated by a "transition-state" surface: in order to go from one (meta) stable state to the other, the system has to cross a free-energy barrier. We assume that the transition state is given by the saddle-point in the free-energy surface $\Delta G(p,n,c)$, as shown in Fig. 3. This means that both the location and the height of the free-energy barrier for flipping are determined by that number n^* for which the two states become equally stable, $\Delta G(p,n^*) = 0$ (see Fig. 3 and Eq. 7). Clearly, the location of the transition state depends upon the phosphorylation level p of the hexamer: in the symmetric model considered here, the two conformational states are equally stable if the number of bound nucleotides is $n^* = p$ (see Fig. 4 and Eq. 7). The height of flipping from the active to inactive state is thus given by

$$\beta\Delta G^*_{\rm A\to I}(p) = -\ln\left[\sum_{q,r} Z^{\rm A}(p,q,r)\delta(q+r-p)/Z^{\rm A}(p,0,6)\right], \tag{8}$$

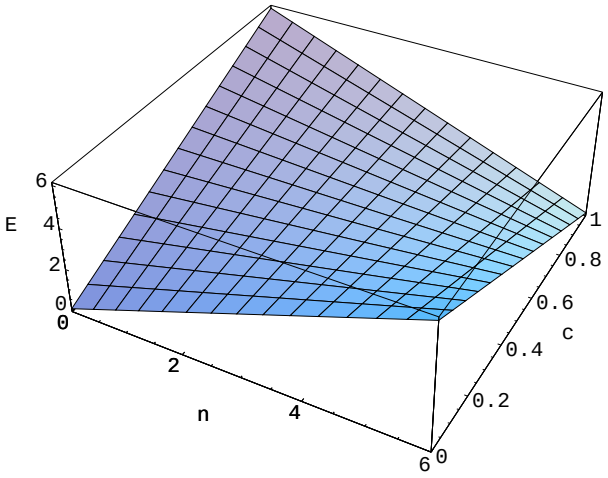

Figure 3: The free energy of a KaiC hexamer for a phosphorylation level of $p = 3$, as a function of the number of bound nucleotides n and as a function of an order parameter c that denotes the conformational state of the KaiC hexamer: it is zero if the hexamer is in the inactive state and one if it is in the active state. In the inactive state, essentially no nucleotides are bound, and $n \approx 0$, while in the actives state, because of strong nucleotide binding, $n \approx 6$. It is seen that in order to flip from the inactive to active state, the system has to cross a free-energy barrier; the transition state is denoted by the red cross. We imagine that the height of the barrier to go from the inactive to active state is given by the free-energy to add three nucleotides, while the barrier to flip from active to inactive is given by the free energy to remove 3 nucleotides.

while the barrier height for the reverse transition is given by

$$\beta \Delta G^*_{\mathrm{I}\to\mathrm{A}}(p) = -\ln\left[\sum_{q,r} Z^{\mathrm{I}}(p,q,r)\delta(q+r-p)/Z^{\mathrm{I}}(p,0,0)\right]. \qquad (9)$$

Here, $Z^{\alpha}(p,q,r)$ is given by Eq. 1. In words, if a p-fold phosphorylated hexamer is in the active state, with 6 nucleotides bound, then in order to flip to the inactive state with no nucleotides bound, it has to cross a barrier with a height that corresponds to the energetic cost of removing $6-p$ nucleotides. Conversely, the height of the barrier for an inactive hexamer, with no nucleotides bound, to flip to the active state, is given by the free energy to add p nucleotides. Neglecting entropic factors, the height of the free-energy barrier thus scales linearly with the phosphorylation level, leading to the exponential flipping rates of Eqs.1 and 2 of the main text.

1.3 Numerical calculations on the allosteric model

The chemical reactions of the model in Fig.1B of the main text are:

$$\mathrm{C}_i \underset{b_i}{\overset{f_i}{\rightleftarrows}} \widetilde{\mathrm{C}}_i, \;\; \mathrm{C}_i \overset{k_{\mathrm{ps}}}{\rightarrow} \mathrm{C}_{i+1}, \;\; \widetilde{\mathrm{C}}_i \overset{\tilde{k}_{\mathrm{dps}}}{\rightarrow} \widetilde{\mathrm{C}}_{i-1} \tag{10}$$

Here, C_i corresponds to an active KaiC hexamer with phosphorylation level i, while $\widetilde{\mathrm{C}}_i$ corresponds to an inactive KaiC hexamer with phosphorylation level i. The first, reversible reaction corresponds to the conformational transitions of the KaiC hexamers with forward and backward flipping rates f_i and b_i, respectively, the second corresponds to phosphorylation of active KaiC at rate k_{ps}, while the third reaction corresponds to dephosphorylation of inactive KaiC at rate $\tilde{k}_{\mathrm{dps}}$.

To study the phosphorylation behavior of a *single* KaiC hexamer, we cannot use macroscopic rate equations based on the law of mass action: these equations would correspond to the average of a *population* of KaiC hexamers. To simulate the behavior of a hexamer, we have performed kinetic Monte Carlo simulations of the zero-dimensional chemical master equation corresponding to the reactions in Eq. 10 [2]. The solid line in Fig.1C corresponds to the results of those stochastic simulations.

To study the time evolution of the average phosphorylation level of an ensemble of KaiC hexamers, we have used macroscopic rate equations based on the law of mass action. The chemical rate equations that correspond to Eq. 10 are:

$$\frac{d[C_i]}{dt} = k_{\mathrm{ps}}[C_{i-1}] - k_{\mathrm{ps}}[C_i] + b_i[\widetilde{C}_i] - f_i[C_i] \tag{11}$$

$$\frac{d[\widetilde{C}_i]}{dt} = \tilde{k}_{\mathrm{dps}}[\widetilde{C}_{i-1}] - \tilde{k}_{\mathrm{dps}}[\widetilde{C}_i] + f_i[C_i] - b_i[\widetilde{C}_i] \tag{12}$$

The dashed line in Fig.1C of the main text corresponds to the numerical results of propagating these ordinary differential equations.

The results in Fig.1C of the main text were obtained with the following values for the parameters: $k_{\mathrm{ps}} = 0.01\mathrm{hr}^{-1}$, $\tilde{k}_{\mathrm{dps}} = 0.05\mathrm{hr}^{-1}$, $f_i = 0.1^{N-i}$ hr^{-1} and $b_i = 0.1^i$ hr^{-1}. We note here that the above chemical rate equations, corresponding to the model in Fig.1B of the main text, are identical to those of the simple model with differential affinity as described in section II with $[\mathrm{A}]_{\mathrm{T}} = 0$ (see Eqs. 17-18). Also the values for the parameters are indentical to those in the differential-affinity model of section II (see section below).

2 Simple Models with Differential Affinity

In this section, we first provide background information on the simplified model of the Kai system discussed in section II of the main text. We then briefly discuss a more generic class of differential affinity models.

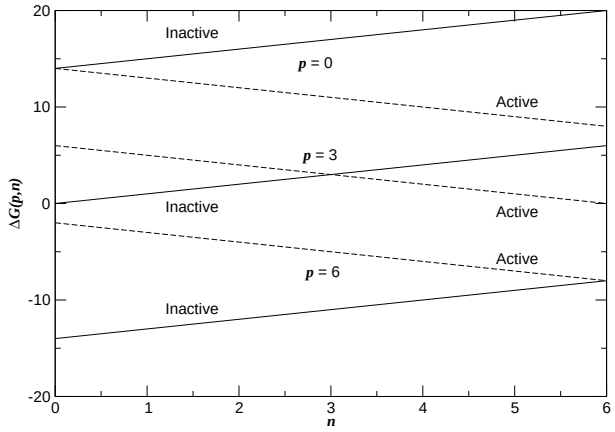

Figure 4: The free energy of the active and inactive state as a function of the number of bound nucleotides, n, for three different phosphorylation levels, $p = 0, 3, 6$. In the active state, $n \approx 6$, while in the inactive state, $n \approx 0$. The free energy of p-fold phosphorylated hexamer in state α with n nucleotides bound is given by $\Delta G^{\alpha}(p,n) = -k_{\rm B}T \ln \sum_{q,r} Z^{\alpha}(p,q,r)\delta(q+r-n)$, where $Z^{\alpha}(p,q,r)$ is given by Eq. 1.

2.1 A minimal differential affinity model of the Kai system

In the simple differential affinity model of section II of the main text, we assume that only a single KaiA dimer can bind to an active KaiC hexamer. The chemical reactions of this model are given in Eqs.3-5 of the main text. They correspond to the following mass-action kinetic equations for the concentrations $[{\rm C}_i]$ and $[\widetilde{\rm C}_i]$ of KaiC in the active and inactive states, $[{\rm AC}_i]$ of the KaiA-KaiC complex, and [A] of free KaiA:

$$\begin{aligned}
\frac{d[{\rm C}_i]}{dt} &= k_{\rm pf}[{\rm AC}_{i-1}] - k^{\rm Af}[{\rm A}][{\rm C}_i] + k_i^{\rm Ab}[{\rm AC}_i] \\
&\quad +\delta_{i,0} b_0 [\widetilde{\rm C}_0] - \delta_{i,6} f_6 [{\rm C}_6] \qquad (13)\\
\frac{d[{\rm AC}_i]}{dt} &= -k_{\rm pf}[{\rm AC}_i] + k^{\rm Af}[{\rm A}][{\rm C}_i] - k_i^{\rm Ab}[{\rm AC}_i] \quad (i \neq 6) \qquad (14)\\
\frac{d[\widetilde{\rm C}_i]}{dt} &= \tilde{k}_{\rm dps}([\widetilde{\rm C}_{i-1}] - [\widetilde{\rm C}_i]) - \delta_{i,0} b_0 [\widetilde{\rm C}_0] + \delta_{i,6} f_6 [{\rm C}_6] \qquad (15)\\
\frac{d[{\rm A}]}{dt} &= -[{\rm A}] \sum_{i=0}^{5} k_i^{\rm Af}[{\rm C}_i] + \sum_{i=0}^{5} (k_i^{\rm Ab} + k_{\rm pf})[{\rm AC}_i] \,, \qquad (16)
\end{aligned}$$

where $\delta_{i,j}$ is the Kronecker delta, $\tilde{k}_{\rm dps}$ is the spontaneous dephosphorylation rate, $k_{\rm pf}$ is the rate of phosphorylation catalyzed by KaiA, and f_i and b_i are the flipping rates as defined in Eqs.1 and 2 of the main text. The rates of KaiA binding to and unbinding from active KaiC are respectively $k^{\rm Af}$ and $k_i^{\rm Ab}$, with

the latter dependent on the number of i of phosphorylated monomers in the KaiC hexamer. Because we generally choose parameters such that (un)binding of KaiA to KaiC is much faster than (de)phosphorylation, it is an excellent approximation to assume that these binding reactions are equilibrated. In this case, we do not have to keep track of $[\mathrm{C}_i]$ and $[\mathrm{AC}_i]$ separately; instead, we obtain dynamical equations for the total concentration $[\mathrm{C}_i]_\mathrm{T} = [\mathrm{C}_i] + [\mathrm{AC}_i]$ of KaiC in the active state and for $[\widetilde{\mathrm{C}}_i]$:

$$\begin{aligned}\frac{d[\mathrm{C}_i]_\mathrm{T}}{dt} &= \frac{k_\mathrm{pf}[\mathrm{A}]}{K_{i-1}+[\mathrm{A}]}[\mathrm{C}_{i-1}]_\mathrm{T} - \frac{k_{pf}[\mathrm{A}]}{K_i+[\mathrm{A}]}[\mathrm{C}_i]_\mathrm{T} \\ &\quad +\delta_{i,0}b_i[\widetilde{\mathrm{C}}_i] - \delta_{i,6}f_i[\mathrm{C}_i]_\mathrm{T} \qquad (17)\\ \frac{d[\widetilde{\mathrm{C}}_i]}{dt} &= \tilde{k}_\mathrm{dps}([\widetilde{\mathrm{C}}_{i-1}] - [\widetilde{\mathrm{C}}_i]) - \delta_{i,0}b_i[\widetilde{\mathrm{C}}_i] + \delta_{i,6}f_i[\mathrm{C}_i]_\mathrm{T} \qquad (18)\end{aligned}$$

along with a constraint equation giving the free KaiA concentration [A] implicitly:

$$[\mathrm{A}] + \sum_i \frac{[\mathrm{A}][\mathrm{C}_i]_\mathrm{T}}{K_i + [\mathrm{A}]} = [\mathrm{A}]_\mathrm{T}. \qquad (19)$$

Here $[\mathrm{A}]_\mathrm{T}$ is the total concentration of KaiA and $K_i = k_i^\mathrm{Ab}/k^\mathrm{Af}$ is the dissociation constant for KaiA binding to i-fold phosphorylated KaiC in the active state. We implement differential affinity by setting $K_i = \beta\alpha^i$ with $\alpha > 1$. Here, and in the next section, the differential equations were solved using Matlab. We note that the assumption that KaiA binding is fast is convenient for some purposes but not essential; we have verified that the model's predictions are the same whether we use Eqs. 13–16 or the reduced set Eqs. 17–19.

PARAMETER VALUES GO HERE (or probably, better yet, in a table).

2.2 Parameter dependence and bifurcation behavior

It is natural to ask how the model's behavior changes as the parameters are varied from the specific values listed in the previous subsection**OR: IN THE TABLE**. This task is facilitated by its simple cyclic structure, which allows one to prove that the system of equations 13–16 always admits exactly one fixed point. As the total concentration $[\mathrm{A}]_\mathrm{T}$ of KaiA is increased from zero, this fixed point becomes unstable through a supercritical Hopf bifurcation. The resulting stable limit cycle persists through a fairly broad range of $[\mathrm{A}]_\mathrm{T}$ values before finally disappearing at a second supercritical Hopf bifurcation where the unique fixed point regains its stability. This behavior can be understood based on arguments similar to those put forth in Section IIIC of the main text: If $[\mathrm{A}]_\mathrm{T}$ is too large, then the concentration of KaiA is no longer limiting, and differential affinity cannot act to synchronize oscillations. On the other hand, if $[\mathrm{A}]_\mathrm{T}$ beocmes too small (while the other parameters are held fixed), then the phosphorylation reactions will proceed too slowly compared to the dephosphorylation reactions. The first phosporylated hexamers will then be dephosphorylated and return to

state C_0 before the remaining KaiC complexes reach state C_6; the hexamers in state C_0 will win the competition for the limited KaiA, preventing the synchronized release of the remainder of the KaiC. Varying other parameters has similar effects. For example, as the parameter β in $K_i = \beta\alpha^i$ is increased, the limit cycle will eventually collapse into the fixed point in a Hopf bifurcation. Indeed, if the K_i become too large, then KaiC hexamers cannot efficiently bind all of the available KaiA, and differential affinity is no longer possible. Figure **??** shows a 2-parameter bifurcation diagram as a function of $[A]_T$ and β. We will see that similar bifurcation behavior reappears in more realistic models of the Kai system.

2.3 Generic differential affinity model

The simple model discussed above and in Section II of the main text can be seen as one example of a more generic class of models that use the same mechanism to synchronize oscillations. Here, we briefly discuss this broader perspective on differential affinity. A fuller mathematical analysis will appear in a forthcoming publication.

We begin by considering the following cycle:

$$C_0 \xrightarrow{k_0} C_1 \xrightarrow{k_1} \ldots \rightarrow C_{N-1} \rightarrow C_N \xrightarrow{k_N} C_0, \tag{20}$$

where C_i is a protein that has been i-fold covalently modified. At least two of the reactions require a catalyst A acting with Michaelis-Menten kinetics, and those steps that are not catalyzed by A are simple first-order reactions.

Suppose that the reactions $C_0 \rightarrow C_1 \rightarrow \ldots \rightarrow C_j$ require the catalyst A (with $j < N$). Then, one might imagine that this system will oscillate if a) the concentration of A is sufficiently low and b) if the dissociation constants K_i for the binding of A to C_i satisfy $K_0 < K_1 < \ldots < K_j$. These two conditions together ensure that A first binds to C_0 and catalyzes the reaction $C_0 \rightarrow C_1$; only when the concentration of C_0 has dropped almost to zero does A begin to bind to C_1 and catalyze the next reaction, and so on until state C_j is reached. It turns out, however, that these requirements alone are not sufficient. In addition, we must demand that c) the distribution of arrival times of different C molecules at C_j is not too wide compared to the average time to travel from C_j back to C_0 and d) that the distribution of arrival times back at C_0 is not too broad. If the former condition, c), does not hold, then the fastest C molecules will reach C_0 while some of the slower C molecules have still not reached C_j. As we noted in the previous subsection, oscillations cannot survive such a situation: Because A binds most strongly to C_0, the fastest C molecules will siphon away A from the slowest that still need A to progress around the cycle; these will then slow down further until all sychronizing effect of differential affinity has been lost. Similarly, differential affinity fails when the arrival of C molecules at state C_0 is too spread out. Then, there are relatively few C's competing for A molecules at any given instant, and even those with the highest number i of modifications can continue upwards towards C_j. Thus, for oscillations to occur, $N - j$ must be neither too small nor too large.

We have succeeded in finding limit cycles in this model with j as small as 1 (corresponding to A binding to the two states C_0 and C_1) and N as small as 4. Fig **??** shows oscillations in such a model with **PARAMETER VALUES HERE**. Although the oscillations persist only up to $N = 7$ for these same parameter values, there appears to be no maximum allowed value of N if the rate k_{ps} of the transitions $C_j \to C_{j+1} \to \ldots \to C_N \to C_0$ is allowed to decrease as $1/(N-j)$. Indeed, in this case, the mean time to travel from C_j to C_0 remains constant, while the distribution of travel times becomes narrower, which only enhances oscillations.

One could imagine many variations on the model just described. For example, we anticipate that for appropriate parameter values, oscillations will also occur when A binds to and is sequestered by C_0 but is not required for the transition $C_0 \to C_1$, while still catalyzing the reaction $C_1 \to C_2$. One might also consider cases in which differential affinity acts on two separated blocks of reactions $C_0 \to C_1 \to \ldots \to C_j$ and $C_n \to C_{n+1} \to \ldots \to C_{n+k}$. In each case, the same basic principles of differential affinity should be at work.

The models of the Kai system in the main text are related to this generic class of models. The phosphorylation cycles of both the minimal differential affinity model of section II and of the full model of the Kai system in section III have an active branch where KaiC is phosphorylated, and an inactive branch where KaiC is dephosphorylated. Also in both models, KaiA catalyzes the phosphorylation reactions on the active branch. Both ingredients are inspired by experimental observations; together they give a concrete example of how the abstract cycle of Eq. 20 might be implemented. However, the discussion of the generic model above shows that from the perspective of synchronising the oscillations, there is no need to make a distrinction between an active and an inactive branch. Indeed, the same formalism could be applied to cycles made of more than two allosteric conformations, or of multiple different sorts of covalent modifications, or created in any number of other ways. The differential affinity mechanism thus has the potential to be generalized far beyond the Kai system.

3 Full Model of the Kai System

3.1 Model: the chemical rate equations

The chemical reactions that describe the full model of the Kai system are given by Eqs.7-11 of the main text. Using the law of mass action, this leads to the following set of macroscopic chemical rate equations for the concentration of $[C_i]$, $[AC_i]$, $[\widetilde{C}_i]$, $[B_m\widetilde{C}_i]$, and $[A_mB_m\widetilde{C}_i]$:

$$
\begin{aligned}
\frac{d[\mathrm{C}_i]}{dt} &= k_{\mathrm{ps}}[\mathrm{C}_{i-1}]+k_{\mathrm{dps}}[\mathrm{C}_{i+1}]-(k_{\mathrm{ps}}+k_{\mathrm{dps}})[\mathrm{C}_i]+k_{\mathrm{pf}}[\mathrm{AC}_{i-1}] \\
&\quad -f_i[\mathrm{C}_i]+b_i[\widetilde{\mathrm{C}}_i]-k_i^{\mathrm{Af}}[\mathrm{A}][\mathrm{C}_i]+k_i^{\mathrm{Ab}}[\mathrm{AC}_i] \qquad (21)\\
\frac{d[\mathrm{AC}_i]}{dt} &= k_i^{\mathrm{Af}}[\mathrm{A}][\mathrm{C}_i]-k_i^{\mathrm{Ab}}[\mathrm{AC}_i]-k_{\mathrm{pf}}[\mathrm{AC}_{i-1}] \qquad (22)\\
\frac{d[\widetilde{\mathrm{C}}_i]}{dt} &= \tilde{k}_{\mathrm{ps}}[\widetilde{\mathrm{C}}_{i-1}]+\tilde{k}_{\mathrm{dps}}[\widetilde{\mathrm{C}}_{i+1}]-(\tilde{k}_{\mathrm{ps}}+\tilde{k}_{\mathrm{dps}})[\widetilde{\mathrm{C}}_i]+f_i[\mathrm{C}_i]-b_i[\widetilde{\mathrm{C}}_i] \\
&\quad -\tilde{k}_i^{\mathrm{Bf}}[\mathrm{B}]^m[\widetilde{\mathrm{C}}_i]+\tilde{k}_i^{\mathrm{Bb}}[\mathrm{B}_m\widetilde{\mathrm{C}}_i] \qquad (23)\\
\frac{d[\mathrm{B}_m\widetilde{\mathrm{C}}_i]}{dt} &= \tilde{k}_{\mathrm{ps}}[\mathrm{B}_m\widetilde{\mathrm{C}}_{i-1}]+\tilde{k}_{\mathrm{dps}}[\mathrm{B}_m\widetilde{\mathrm{C}}_{i+1}]-(\tilde{k}_{\mathrm{ps}}+\tilde{k}_{\mathrm{dps}})[\mathrm{B}_m\widetilde{\mathrm{C}}_i] \\
&\quad +\tilde{k}_i^{\mathrm{Bf}}[\mathrm{B}]^m[\widetilde{\mathrm{C}}_i]-\tilde{k}_i^{\mathrm{Bb}}[\mathrm{B}_m\widetilde{\mathrm{C}}_i] \\
&\quad -\tilde{k}_i^{\mathrm{Af}}[\mathrm{A}]^m[\mathrm{B}_m\widetilde{\mathrm{C}}_i]+\tilde{k}_i^{\mathrm{Ab}}[\mathrm{A}_m\mathrm{B}_m\widetilde{\mathrm{C}}_i] \qquad (24)\\
\frac{d[\mathrm{A}_m\mathrm{B}_m\widetilde{\mathrm{C}}_i]}{dt} &= \tilde{k}_{\mathrm{ps}}[\mathrm{A}_m\mathrm{B}_m\widetilde{\mathrm{C}}_{i-1}]+\tilde{k}_{\mathrm{dps}}[\mathrm{A}_m\mathrm{B}_m\widetilde{\mathrm{C}}_{i+1}]-(\tilde{k}_{\mathrm{ps}}+\tilde{k}_{\mathrm{dps}})[\mathrm{A}_m\mathrm{B}_m\widetilde{\mathrm{C}}_i] \\
&\quad +\tilde{k}_i^{\mathrm{Af}}[\mathrm{A}]^m[\mathrm{B}_m\widetilde{\mathrm{C}}_i]-\tilde{k}_i^{\mathrm{Ab}}[\mathrm{A}_m\mathrm{B}_m\widetilde{\mathrm{C}}_i] \qquad (25)
\end{aligned}
$$

Here, the concentrations of free KaiA and KaiB, [A] and [B], are given by:

$$
\begin{aligned}
[\mathrm{A}] &= [\mathrm{A}]_{\mathrm{T}}-\sum_{i=0}^{N}([\mathrm{AC}_i]+m[\mathrm{A}_m\mathrm{B}_m\widetilde{\mathrm{C}}_i]) \qquad (26)\\
[\mathrm{B}] &= [\mathrm{B}]_{\mathrm{T}}-\sum_{i=0}^{N}(m[\mathrm{B}_m\widetilde{\mathrm{C}}_i]+m[\mathrm{A}_m\mathrm{B}_m\widetilde{\mathrm{C}}_i]) \qquad (27)
\end{aligned}
$$

The phosphorylation and dephosphorylation rates on the active branch are k_{ps} and k_{dps}, respectively, and the flipping rates are f_i and b_i. The active state can bind KaiA with forward and backward rates k_i^{Af} and k_i^{Ab}, and KaiA can catalyze phosphorylation with the rate k_{pf}. We assume that in the inactive state KaiC can bind $m=2$ KaiB molecules with forward and backward rates $\tilde{k}_i^{\mathrm{Bf}}$ and $\tilde{k}_i^{\mathrm{Bb}}$, respectively. This KaiB-KaiC complex can then sequester $m=2$ KaiA molecules with forward and backward rates $\tilde{k}_i^{\mathrm{Af}}$ and $\tilde{k}_i^{\mathrm{Ab}}$.

3.2 Model: The free-energy difference between the active and inactive state of KaiC

In the presence of only KaiA, KaiC is phosphorylated to a very high level of $90-95\%$. This requires that the active state of KaiC be more stable than the inactive one. However, in order for KaiC to sustain oscillations in the presence of both KaiA and KaiB, KaiC should be able to flip from the active state to the inactive one at higher phosphorylation levels. This means that the free-energy difference $\Delta G(p)$ between KaiC in its active and inactive conformational

$k_{\rm ps}$, $\tilde{k}_{\rm ps}$	$0.025\ \mathrm{hr}^{-1}$
$k_{\rm dps}$, $\tilde{k}_{\rm dps}$	$0.4\ \mathrm{hr}^{-1}$
$k_{\rm pf}$	$1.0\ \mathrm{hr}^{-1}$
f_i	$\{10^{-5}, 10^{-5}, 10^{-4}, 10^{-3}, 10^{-2}, 10^{-1}, 10\}\ \mathrm{hr}^{-1}$
b_i	$100\ \mathrm{hr}^{-1}$
$k_i^{\rm Af}$	$1.72{\cdot}10^{6}\ \mathrm{M}^{-1}\mathrm{hr}^{-1}$
$k_i^{\rm Ab}$	$\{10, 30, 90, 270, 810, 2430, 7290\}\ \mathrm{hr}^{-1}$
$\tilde{k}_i^{\rm Bf}$	$2.97{\cdot}10^{12} \times \{0.01, 1, 1, 1, 1, 1, 1\}\ \mathrm{M}^{-2}\mathrm{hr}^{-1}$
$\tilde{k}_i^{\rm Bb}$	$1{\cdot}10^{2} \times \{10, 1, 1, 1, 1, 1, 1\}\ \mathrm{hr}^{-1}$
$\tilde{k}^{\rm Af}$	$2.97{\cdot}10^{18} \times \{0, 1, 100, 100, 1, 0, 0\}\ \mathrm{M}^{-2}\mathrm{hr}^{-1}$
$\tilde{k}^{\rm Ab}$	$100\ \mathrm{hr}^{-1}$
$[\mathrm{A}]_{\rm T}$	$0.58\ \mu\mathrm{M}$
$[\mathrm{B}]_{\rm T}$	$1.75\ \mu\mathrm{M}$
$[\mathrm{C}]_{\rm T}$	$0.58\ \mu\mathrm{M}$

Table 1: List of parameter values for the full model in Section III of the main text.

states should be strongly negative, but also that it should rapidly decrease in magnitude as KaiC becomes fully phosphorylated. A simple model that captures this is one in which the addition of each phosphate group decreases the free-energy difference by an amount ΔE_p, and moreover where the creation of an interface between a phosphorylated and an unphosphorylated unit also destabilizes the inactive state by an additional amount ϵ: upon the addition of the last phosphate group, two such interfaces are removed, leading to an extra change in the free-energy difference of 2ϵ in favor of the inactive state. This leads to the following expression for the free-energy difference between the active and inactive state:

$$\Delta G(p, q, r) = N\Delta E_{\rm m} + p\Delta E_p - \epsilon \sum_{\langle i,j \rangle} n_i n_j + q\Delta E_{\rm T} + r\Delta E_{\rm D}. \qquad (28)$$

Here, n_i denotes the phosphorylation state of unit i – $n_i = 1$ if unit i contains a phosphate group and zero otherwise – and the sum $\langle i, j \rangle$ includes all nearest neighbor units of KaiC. For the full model, $\Delta E_{\rm m}, \Delta E_{\rm T}, \Delta E_{\rm D} < 0$, and ΔE_p, $\epsilon > 0$. For simplicity, we assume that $\Delta E_p = 2\epsilon$. This yields the following expressions for the transitions between the active and inactive states: for the forward rate we have $f_i = \delta\gamma^{N-i}$ for $1 \leq i < N$ and $f_i = 10 \cdot \delta\gamma^{N-i}$ for $i = 0, N$ (this is due to, respectively, the creation or removal of the interfaces between phosphorylated and unphosphorylated units). The backward rate b_i is independent of i and much larger than the forward rate f_i, so that the stability of the inactive state is only due to binding of KaiB.

3.3 Setting the parameters

Using the expressions for f_i and b_i just derived, the full model contains 39 parameters. However, their values are very much constrained by the large body of experimental data on this system. We now describe how we have determined the parameters, and how critical their precise values are for the behavior of the model. Unless indicated otherwise, the exact values of the parameters for the full model are summarized in Table 1.

Concentrations The concentrations of KaiA and KaiB dimers are $[\mathrm{A}]_\mathrm{T} = 0.58\mu\mathrm{M}$ and $[\mathrm{B}]_\mathrm{T} = 1.75\mu\mathrm{M}$, respectively, and the concentration of KaiC hexamers is $[\mathrm{C}]_\mathrm{T} = 0.58\mu\mathrm{M}$. This corresponds to a concentration ratio of (KaiA dimers):(kaiB dimers):(KaiC hexamers) = 1:3:1. The corresponding *monomer* concentrations are 1.17μM KaiA, 3.5μM KaiB and 3.5μM KaiC. Oscillations in phosphorylation have been observed for these concentrations in the *in vitro* experiments of Tomita *et al.* [3]. However, it should be noted that for the results in this article the ratios of KaiA and KaiB to KaiC, $[\mathrm{A}]_\mathrm{T}/[\mathrm{C}]_\mathrm{T}$ and $[\mathrm{B}]_\mathrm{T}/[\mathrm{C}]_\mathrm{T}$ respectively, are more important than absolute concentrations. Hence, we often express concentrations in units relative to $[\mathrm{C}]_\mathrm{T}$.

Flipping rates Following the discussion in the last paragraph of the previous section on the model for the free-energy difference between the active and inactive state of the KaiC hexamers, we next discuss the values of the flipping rates. As discussed in that paragraph, it is important that: 1) in the absence of KaiB, the active state has a lower free energy than the inactive one; 2) the hexamers should not flip at intermediate phosphorylation levels. In the previous section, we presented a model for the free-energy difference between the active and inactive state. Here we give the values of the flipping rates that are consistent with this free-energy difference, which is requirement 1), and with requirement 2). The forward rate is $f_i = \delta\gamma^{N-i}$ for $1 \leq i < N$ and $f_i = 10 \cdot \delta\gamma^{N-i}$ for $i = 0, N$, with $\gamma = 0.1$ and $\delta = 2\mathrm{hr}^{-1}$. The backward rate b_i is independent of i and given by $b = 100\mathrm{hr}^{-1}$. As long as the two requirements of this paragraph are satisfied, however, the precise values of the flipping rates are not important for the behavior of the model.

KaiC alone and KaiC + KaiB: Spontaneous (de)phosphorylation rates The spontaneous phosphorylation and dephoshorylation rates are chosen such that the phosphorylation behavior of KaiC in the absence of KaiA and KaiB and that in the presence of only KaiB agrees well with experiment (see Fig. 4 of the main text). This yields the following rates for, respectively, the spontaneous phosphorylation and spontaneous dephosphorylation reactions, both for active and inactive KaiC: $k_\mathrm{ps} = \tilde{k}_\mathrm{ps} = 0.025\mathrm{hr}^{-1}$ and $k_\mathrm{dps} = \tilde{k}_\mathrm{dps} = 0.4\mathrm{hr}^{-1}$. The identical rates for active and inactive KaiC ensure that the phosphorylation behavior of KaiC in the absence of KaiA and KaiB is the same as that of KaiC in the presence of KaiB (which stabilizes the inactive branch). The values of these rate constants are not free and have to be carefully chosen, because their sum determines the relaxation rate of the phosphorylation level of KaiC (in the absence of KaiA), while their ratio determines the steady-state phosphorylation level of KaiC (in the absence of KaiA).

KaiC + KaiA: rates of KaiA-catalyzed phosphorylation reactions The phosphorylation rate of KaiC in the presence of KaiA is determined by two factors: 1) the binding affinity of KaiA for KaiC; 2) the rate $k_{\rm pf}$ for the KaiA-catalyzed phosphorylation reaction. As discussed in the main text, both the mechanism of differential affinity and temperature compensation require that the binding affinities of KaiA for KaiC be high. Given these high binding affinities, the rate at which KaiC is phosphorylated in the presence of KaiA is mostly determined by $k_{\rm pf}$. This rate is thus chosen such that the phosphorylation rate of KaiC in the presence of KaiA agrees with experiment. This gives $k_{\rm pf} = 1{\rm hr}^{-1}$. This rate constant cannot be freely chosen, because it directly affects the phosphorylation rate of KaiC in the presence of KaiA.

The mechanism of differential affinity requires that the affinity of KaiA for KaiC be high, but decrease substantially as the phosphorylation level of KaiC increases. Provided that these constraints are satisfied, the precise values are of less importance. We have chosen the following expressions for the forward rate $k_i^{\rm Af}$ and backward rate $k_i^{\rm Ab}$: $k_i^{\rm Af} = 1.72 \cdot 10^6 {\rm M}^{-1}{\rm hr}^{-1}$ and $k_i^{\rm Ab} = \beta\alpha^i {\rm hr}^{-1}$, with $\alpha = 3$ and $\beta = 10$.

The binding of KaiA and KaiB to inactive KaiC The stoichiometries of the complexes of KaiC bound to KaiB and KaiA are not known. We assume that inactive KaiC, $\widetilde{\rm C}_i$ binds $m = 2$ KaiB dimers, while the complex ${\rm B}_2\widetilde{\rm C}_i$ can sequester $m = 2$ KaiA dimers. The value of $m = 2$ is not very critical, as long as enough KaiA can be sequestered by inactive KaiC the amount of KaiC available to catalyze phosphorylation is limited. We find that for $m > 2$ the system also oscillates, although the phase boundaries, as shown in Fig.6 of the text, do shift. Clearly, more experiments are needed to resolve the compositions of these complexes.

Temperature compensation requires that the binding affinities of KaiB for KaiC be high. But as long as this requirement is fulfilled, the precise values are of less importance. We assume that KaiB binds inactive KaiC with forward rate $k_i^{\rm Bf} = 2.97 \cdot 10^{12} \times \{0.01, 1, 1, 1, 1, 1, 1\}{\rm M}^{-2}{\rm hr}^{-1}$ and backward rate $k_i^{\rm Bb} = 1 \cdot 10^2 \times \{10, 1, 1, 1, 1, 1, 1\}{\rm hr}^{-1}$. The low affinity of KaiB for $\widetilde{\rm C}_0$ is to ensure that unphosphorylated hexamers that are in the inactive state can rapidly flip towards the active state.

As explained in the main text, it is important that the affinity of KaiA for KaiB is low for KaiB associated with the highly phosphorylated inactive KaiC hexamers, but increases strongly for KaiB that is bound to the less-phosphorylated inactive KaiC hexamers; the precise values of the dissociation constants are not critical. We have chosen the following forward rate $\tilde{k}_i^{\rm Af}$ and backward rate $\tilde{k}_i^{\rm Ab}$: $\tilde{k}_i^{\rm Af} = 2.97 \cdot 10^{18} \times \{0, 1, 100, 100, 1, 0, 0\}{\rm M}^{-2}{\rm hr}^{-1}$ and $\tilde{k}_i^{\rm Ab} = 100{\rm hr}^{-1}$. The low affinity of KaiA for ${\rm B}_2\widetilde{\rm C}_0$ is to ensure that unphosphorylated hexamers that are in the inactive state can rapidly flip towards the active state.

Varying the parameters with temperature In order to calculate how the oscillation period in our model varies with temperature, we would have to know how the rate constants would vary with temperature. This would require knowl-

edge of the activation barrier for each of the reactions, which we do not have. We can, however, test how sensitive the oscillation period is to changes in the rate constants. Here, one could choose various strategies: one could vary each of the rate constants individually, or one could vary all the rate constants simultaneously, either in a correlated or an uncorrelated manner. We have performed many such tests, and they all reveal that the model is very robust to changes in temperature (given the experimentally observed insensitivity of the phosphorylation rates to changes in temperature (see main text)). Since the dissociation constants and the flip rates enter the model in very different ways, we show in the main text how the oscillations change when we vary these two groups of parameters.

When we change the dissociation constants of KaiA and KaiB binding to examine the effects of temperature changes, we simultaneously change the dissociation constants for KaiA binding, K_i and $\widetilde{K}_i$, by a factor C, and the association and dissociation rates for KaiB binding, k_i^{Bf} and k_i^{Bb}, by $1/\sqrt{C}$ and $\sqrt{C}$, respectively. Because KaiB (un) binding is fast, only the *ratios* of their rates—the dissociation constants—matter, and this is a choice that is consistent with changing the dissociation constants by a factor C.

3.4 Reduced model

When KaiA binding and unbinding is sufficiently rapid, it is possible to further simplify Eqs. 21-25. In this case, we only explicitly take into account the binding of KaiB to the inactive KaiC hexamers and we assume that both KaiA association to the active KaiC hexamers and KaiA sequestration by KaiB bound to the inactive hexamers is very rapid and can be treated as in chemical equilibrium. This leads to the following reduced set of macroscopic chemical rate equations for the total concentration $[\mathrm{C}_i]_\mathrm{T}$ of KaiC in the active state, both with and without bound KaiA, the concnetration of KaiC in the inactive state, $[\widetilde{\mathrm{C}}_i]$, and the total concentration $[\mathrm{B}_m\widetilde{\mathrm{C}}_i]_\mathrm{T}$ of KaiC in the inactive state with KaiB bound, both with and without bound KaiA:

$$\frac{d[\mathrm{C}_i]_\mathrm{T}}{dt} = \sigma_{i-1}^{\mathrm{ps}}[\mathrm{C}_{i-1}]_\mathrm{T}+\sigma_{i+1}^{\mathrm{dps}}[\mathrm{C}_{i+1}]_\mathrm{T}-(\sigma_i^{\mathrm{ps}}+\sigma_i^{\mathrm{dps}})[\mathrm{C}_i]_\mathrm{T}-\sigma_i^{\mathrm{Ff}}[\mathrm{C}_i]_\mathrm{T}+\sigma_i^{\mathrm{Fb}}[\widetilde{\mathrm{C}}_i] \quad (29)$$

$$\begin{aligned}\frac{d[\widetilde{\mathrm{C}}_i]}{dt} &= \tilde{k}_{\mathrm{ps}}[\widetilde{\mathrm{C}}_{i-1}]+\tilde{k}_{\mathrm{dps}}[\widetilde{\mathrm{C}}_{i+1}]-(\tilde{k}_{\mathrm{ps}}+\tilde{k}_{\mathrm{dps}})[\widetilde{\mathrm{C}}_i]+\sigma_i^{\mathrm{Ff}}[\mathrm{C}_i]_\mathrm{T}-\sigma_i^{\mathrm{Fb}}[\widetilde{\mathrm{C}}_i] \\ &\quad -k_i^{\mathrm{Bf}}([\mathrm{B}]_\mathrm{T}-m\textstyle\sum_i[\mathrm{B}_m\widetilde{\mathrm{C}}_i]_\mathrm{T})^m[\widetilde{\mathrm{C}}_i]+\dfrac{k_i^{\mathrm{Bb}}\widetilde{\mathrm{K}}_i^m[\mathrm{B}_m\widetilde{\mathrm{C}}_i]_\mathrm{T}}{\widetilde{\mathrm{K}}_i^m+[\mathrm{A}]^m} \quad (30)\end{aligned}$$

$$\begin{aligned}\frac{d[\mathrm{B}_m\widetilde{\mathrm{C}}_i]_\mathrm{T}}{dt} &= \tilde{k}_{\mathrm{ps}}[\mathrm{B}_m\widetilde{\mathrm{C}}_{i-1}]_\mathrm{T}+\tilde{k}_{\mathrm{dps}}[\mathrm{B}_m\widetilde{\mathrm{C}}_{+1}]_\mathrm{T}-(\tilde{k}_{\mathrm{ps}}+\tilde{k}_{\mathrm{dps}})[\mathrm{B}_m\widetilde{\mathrm{C}}_i]_\mathrm{T} \\ &\quad +k_i^{\mathrm{Bf}}([\mathrm{B}]_\mathrm{T}-m\textstyle\sum_i[\mathrm{B}_m\widetilde{\mathrm{C}}_i]_\mathrm{T})^m[\widetilde{\mathrm{C}}_i]-\dfrac{k_i^{\mathrm{Bb}}\widetilde{\mathrm{K}}_i^m[\mathrm{B}_m\widetilde{\mathrm{C}}_i]_\mathrm{T}}{\widetilde{\mathrm{K}}_i^m+[\mathrm{A}]^m} \quad (31)\end{aligned}$$

where the concentration of free KaiA, [A], is given by:

$$[\mathrm{A}] + \sum_{i=0}^{N} \frac{[\mathrm{A}][\mathrm{C}_i]_\mathrm{T}}{\mathrm{K}_i + [\mathrm{A}]} + m \sum_{i=0}^{N} \frac{[\mathrm{A}]^m [\mathrm{B}_m \widetilde{\mathrm{C}}_i]_\mathrm{T}}{\widetilde{\mathrm{K}}_i^m + [\mathrm{A}]^m} - [\mathrm{A}]_\mathrm{T} = 0 \tag{32}$$

The effective (de)phosphorylation rates on the active branch are given by $\sigma_i^{\mathrm{ps}} = (k_{\mathrm{ps}}\mathrm{K}_i + k_{\mathrm{pf}}[\mathrm{A}])/(\mathrm{K}_i + [\mathrm{A}])$ and $\sigma_i^{\mathrm{dps}} = \mathrm{K}_i k_{\mathrm{dps}}/(\mathrm{K}_i + [\mathrm{A}])$. The dissociation constants K_i and $\widetilde{\mathrm{K}}_i$ are given by $\mathrm{K}_i = k_i^{\mathrm{Ab}}/k_i^{\mathrm{Af}}$ and $\widetilde{\mathrm{K}}_i = \tilde{k}_i^{\mathrm{Ab}}/\tilde{k}_i^{\mathrm{Af}}$. The effective flipping rates are given by $\sigma_i^{Ff} = f_i K_i/(K_i + [A])$ and $\sigma_i^{Fb} = b_i$, where f_i and b_i are the forward and backward flipping rates. We have confirmed that for sufficiently large $k^{\mathrm{Af}}, k^{\mathrm{Ab}}$ and $\tilde{k}^{\mathrm{Af}}, \tilde{k}^{\mathrm{Ab}}$ this set of rate equations gives results that are identical to those in Eqs. 21-25. Unless indicated otherwise, the results in the main text are obtained by numerically solving Eqs. 29-31.

3.5 Bifurcation analysis

We have performed a bifurcation analysis of the full model. To this end, we use Eqs. 21-25. However, the system of differential equations in Eqs. 21-25 obeys the conservation law $\sum([\mathrm{C}_i] + [\mathrm{AC}_i] + [\widetilde{\mathrm{C}}_i] + [\mathrm{B}_m\widetilde{\mathrm{C}}_i] + [\mathrm{A}_m\mathrm{B}_m\widetilde{\mathrm{C}}_i]) = [\mathrm{C}]_\mathrm{T}$. As a consequence, a linear stability analysis would always yield at least one eigenvector with eigenvalue zero, which complicates detection of bifurcation points. To eliminate the zero eigenvalue associated with the conservation of KaiC, we express the concentration of one of the KaiC complexes in terms of the concentrations of the other KaiC complexes. We have chosen $[\mathrm{AC}_N]$ to take this role. Thus, $[\mathrm{AC}_N]$ is not a separate dynamical variable, but is instead defined by:

$$[\mathrm{AC}_N] = [\mathrm{C}]_\mathrm{T} - \sum_{i=0}^{N-1} [\mathrm{AC}_i] - \sum_{i=0}^{N} ([\mathrm{C}_i] + [\widetilde{\mathrm{C}}_i] + [\mathrm{B}_m\widetilde{\mathrm{C}}_i] + [\mathrm{A}_m\mathrm{B}_m\widetilde{\mathrm{C}}_i]) \tag{33}$$

Numerical continuation of the fixed points and limit cycles was performed with the software package XPPAUT [4], which incorporates the numerical continuation routines from AUTO [5].

In Fig. 5 we show the bifurcation diagram of the full model, defined by Eqs. 21-25, as a function of $[\mathrm{A}]_\mathrm{T}$, for different values of $[\mathrm{B}]_\mathrm{T}$; the phase diagram is shown in Fig. 6. For very small KaiB concentration, $[\mathrm{B}]_\mathrm{T} < 0.05[\mathrm{C}]_\mathrm{T}$, the system has a single, stable fixed point for all $[\mathrm{A}]_\mathrm{T}$ (Fig. 5). For higher KaiB concentration, $0.05 < [\mathrm{B}]_\mathrm{T}/[\mathrm{C}]_\mathrm{T} < 0.6$, the system is bistable for a range of $[\mathrm{A}]_\mathrm{T}$ (see Figs. 5 and 6): it has two stable steady states and one unstable steady state, corresponding to different degrees of KaiC phosphorylation. At the boundaries of this bistable region, a stable and unstable fixed point merge via a saddle-node bifurcation (Fig. 5). We discuss the origin of this bistable regime in more detail below. For even higher KaiB concentration, $0.6 < [\mathrm{B}]_\mathrm{T}/[\mathrm{C}]_\mathrm{T} < 1.2$, one of the two stable fixed points, namely that with the lower phosphorylation level, becomes unstable for a range of KaiA concentrations. This stable fixed point becomes unstable via a supercritical Hopf bifurcation and gives rise to a limit

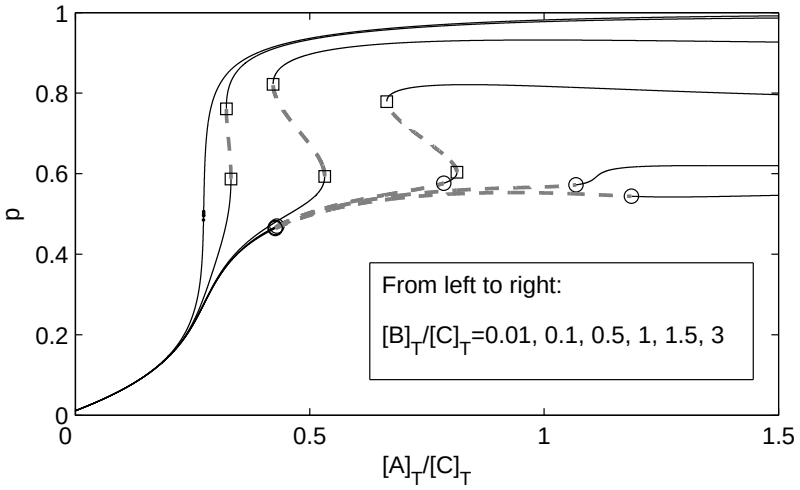

Figure 5: Bifurcation diagram of the full model of Eqs. 21–25 as a function of $[A]_T$, for different values of $[B]_T$. Stable fixed points and unstable fixed points are indicated by solid black lines and dashed grey lines, respectively. When the fixed points change stability, either saddle-node bifurcations (squares) or Hopf bifurcations (circles) occur. Apart from $[A]_T$ and $[B]_T$, all other parameters are as shown in Table 1.

cycle. Thus, in this window of KaiA and KaiB concentrations, the system has one stable fixed point at high phosphorylation level and a limit cycle. For yet larger KaiB concentrations, $[B]_T > 1.2[C]_T$, the system has only one unstable fixed point surrounded by a limit cycle for a range of $[A]_T$; again, the limit cycle appears and disappears at low and high $[A]_T$, respectively, via a supercritical Hopf bifurcation. This limit cycle corresponds to the circadian oscillations discussed in the main text. Fig. 6 shows that this oscillatory regime with only one limit cycle has a lower and an upper bound on the KaiA concentration, but no apparent upper limit on the KaiB concentration. In contrast, both the bistable regime and the regime in which a limit cycle coexists with a stable fixed point, occur only over a fairly narrow range of KaiA and KaiB concentrations.

In Fig. 7, we examine the properties of the limit cycle that is created at the Hopf bifurcation. It is possible to do numerical continuation of the limit cycle in the vicinity of the Hopf bifurcation as is shown in Fig. 7A. This analysis shows that the limit cycle is stable and that the bifurcation is thus supercritical. Further away from the Hopf bifurcation the numerical continuation algorithm fails to converge. However, as shown in Fig. 7B and C, by directly solving the differential equations 21–25 we can nonetheless show that the system continues to converge to a stable limit cycle. Because of the fact that the algorithm cannot continue the limit cycle all the way from one Hopf bifurcation to the other, we cannot strictly rule out the possibility that it undergoes further bifurcations.

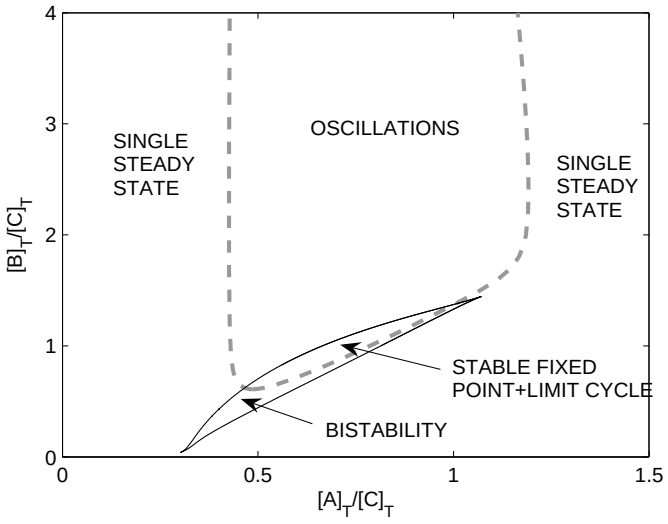

Figure 6: Phase diagram of the full model. In the region enclosed by the dashed grey lines, the system possesses a stable limit cycle. In the region enclosed by the solid black lines, the system has three fixed points, of which two are stable in the absence of a limit cycle. Where the two regions overlap, a single stable fixed point coexists with a limit cycle.

Nevertheless, we find by direct integration of the differential equations that both the period and amplitude of the limit cycle vary smoothly with $[\mathrm{A}]_\mathrm{T}$ between the Hopf bifurcations.

We now discuss the origin of bistability for intermediate $[\mathrm{A}]_\mathrm{T}$ and $[\mathrm{B}]_\mathrm{T}$ (see Fig. 6). Fig. 8 shows four typical time traces of the phosphorylation level of KaiC when the system is in the bistable regime. The different time traces correspond to different initial conditions. These initial conditions differ in the phosphorylation level of KaiC. Indeed, the initial degree of phosphorylation largely determines which one of the stable fixed points the system converges to. For low initial phosphorylation, the system converge to a steady-state phosphorylation level of $p_\mathrm{s} = 0.5$, while for high initial phosphorylation, it converges to a phosphorylation level of $p_\mathrm{s} = 0.9$. These two steady states do not only differ in the average phosphorylation level of KaiC, but, importantly, also in the concentration of *free* KaiA: for $p_\mathrm{s} = 0.5$, [A] is small, while for $p_\mathrm{s} = 0.9$, [A] is large.

To understand the origin of the difference between the two steady states, it should be realized that: a) KaiB is needed to stabilize inactive KaiC, but its concentration is fairly low; b) KaiA is needed to phosphorylate active KaiC, but also its concentration is fairly low.

In the low p_s state, most KaiC hexamers have initially a low degree of phosphorylation. These hexamers will bind KaiA, which will stimulate their

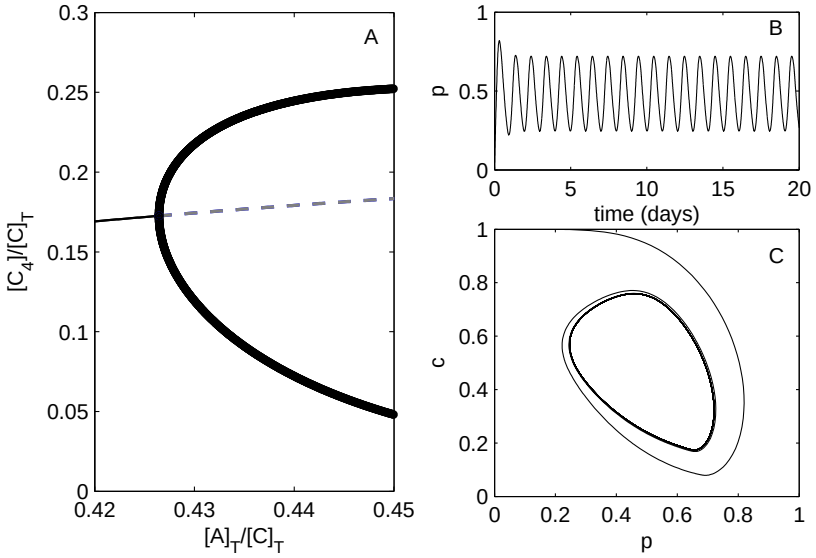

Figure 7: Limit cycle in the full model for $[\mathrm{B}]_\mathrm{T}/[\mathrm{C}]_\mathrm{T} = 3$. (A) Bifurcation diagram of $[\mathrm{C}_4]$ in the vicinity of the Hopf bifurcation as obtained by numerical continuation of the limit cycle. The stable and unstable fixed points are indicated by a solid black line and a dashed grey line, respectively. The minimum and maximum values of $[\mathrm{C}_4]$ along the limit cycle are shown as thick black lines. The limit cycle is stable, indicating a supercritical Hopf bifurcation. Here, we choose to plot $[C_4]$ for convenience, and the concentrations of other components of the system show similar behavior close to the Hopf bifurcation. (B) and (C) Limit cycle for $[\mathrm{A}]_\mathrm{T}/[\mathrm{C}]_\mathrm{T} = 1$ and $[\mathrm{B}]_\mathrm{T}/[\mathrm{C}]_\mathrm{T} = 3$, obtained by numerical integration of Eqs. 21-25. (B) Phosphorylation p in time. (C) Phosphorylation p versus c, the fraction of KaiC in the active state.

phosphorylation. However, because $[\mathrm{A}]_\mathrm{T}$ is low, the phosphorylation rate per hexamer will be low and counterbalanced by the spontaneous dephosphorylation rate. As a consequence, the overall phosphorylation level will be low.

In the high p_s state, most KaiC hexamers go through the approximate cycle $\mathrm{AC}_5 \rightarrow \mathrm{C}_6 \rightarrow \mathrm{B}_2\widetilde{\mathrm{C}}_6 \rightarrow \mathrm{B}_2\widetilde{\mathrm{C}}_5 \rightarrow \mathrm{AC}_5$. In the high p_s state, most KaiC hexamers initially have a high degree of phosphorylation. The available KaiA dimers will be able to fully phosphorylate these hexamers before they flip towards the inactive state. On the inactive branch, these hexamers need KaiB to be stabilized. However, because $[\mathrm{B}]_\mathrm{T}$ is low, the inactive hexamers will not be stabilized very strongly, and will therefore flip back towards the active state. At this point, the concentration of free KaiA is still high, because there are no hexamers with a low phosphorylation level, which could bind KaiA. Because the concentration of free KaiA is high, the hexamers that have just flipped back

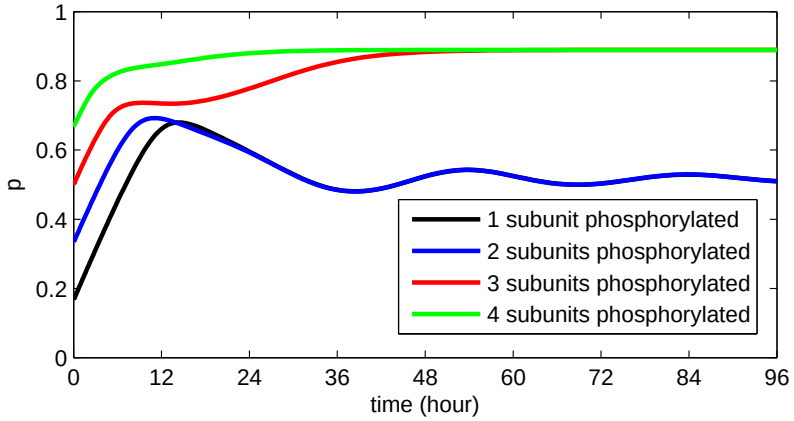

Figure 8: Bistability in the full model for $[\mathrm{A}]_\mathrm{T}/[\mathrm{C}]_\mathrm{T} = 0.48$ and $[\mathrm{B}]_\mathrm{T}/[\mathrm{C}]_\mathrm{T} = 0.5$. The degree of phosphorylation in time is shown for different initial conditions, $[\mathrm{C}_i(0)] = [\mathrm{C}]_\mathrm{T}$ for $i = 1, 2, 3, 4$. For low initial phosphorylation, the system converges to a steady state at $p \approx 0.5$. For high initial phosphorylation the system converges to another steady state at $p \approx 0.9$.

towards the active state can be rephosphorylated, and the cycle starst again. This situation clearly elucidates the important role of KaiB. Without KaiB the inactive branch is not stable, and the full allosteric cycle will be short cut. This will kill the capacity of the system to generate macroscopic oscillations.

The above mechanism for generating bistability is similar to the mechanisms that have been proposed for generating bistability in the MAPK [6] and the CAMKII system [7]. Both in these systems and in the Kai system, a protein can be phosphorylated at multiple sites and the limiting amount of either the kinase, as in the Kai or the MAPK system, or the limiting amount of phosphatase, as in the CAMKII system, makes the system flip-flop between a state with a high phosphorylation level and one with a low phosphorylation level.

Fig. 6 summarizes the behavior of the full system. The full model has a limit cycle for a broad range of concentrations. Although the range of $[\mathrm{A}]_\mathrm{T}$ for which oscillations are observed decreases slightly with increasing $[\mathrm{B}]_\mathrm{T}$, we found no indication that oscillations cease for higher $[\mathrm{B}]_\mathrm{T}$. This is in agreement with the passive role played by KaiB in stabilizing the inactive branch and sequestering KaiA. The region for which bistability occurs is much smaller. Furthermore, as we have discussed above, the occurrence of the bistable regime does depend upon details of the model, such as the extent to which KaiB sequesters KaiA and stabilizes the inactive state when bound to KaiC. Further experiments will be needed to determine whether bistability really occurs in the Kai system.

References

[1] Chandler, D. *Introduction to modern statistical mechanics*, Oxford University Press, New York (1987).

[2] Gillespie, D. T. (1977) *J. Phys. Chem.* **81**, 2340-2361.

[3] Kageyama, H., Nishiwaki, T., Nakajima, M., Iwasaki, H., Oyama, T. & Kondo, T., (2006) *Moll. Cell* **23**, 161-171.

[4] Ermentrout, B. *Simulating, Analyzing, and Animating Dynamical Systems*, Society for Industrial and Applied Mathematics, Philadelphia (2002).

[5] Doedel, E., R. Paffenroth, A. Champneys, T. Fairgrieve, Y. Kuznetsov, B. Sandstede, and X. Wang. *AUTO 2000: Continuation and bifurcation software for ordinary differential equations (with HOMCONT).* Technical report. Caltech, Pasadena, CA (2001).

[6] Markevich, N. I., Hoek, J. B., and Kholodenko, B. N. (2004) *J. Cell Biol.* **164**, 353 - 359.

[7] Miller, P. Zhabotinsky, A.M., Lisman, J.E., Wang, X.J., *PLoS Biology* **3**, 705-717.